Supporting Information

Precise Control of CNT-DNA Assembled Nanomotor Using Oppositely Charged Dual Nanopores

Chaofan Ma,[a,b] Wei Xu[a,b], Wei Liu[a,b], Changhui Xu[a,b], Wei Si*[a,b] and Jingjie Sha*[a,b]

[a]School of Mechanical Engineering, Southeast University, Nanjing, China.

[b]Jiangsu Key Laboratory for Design and Manufacture of Micro-nano Biomedical Instruments, Southeast University, Nanjing, China.

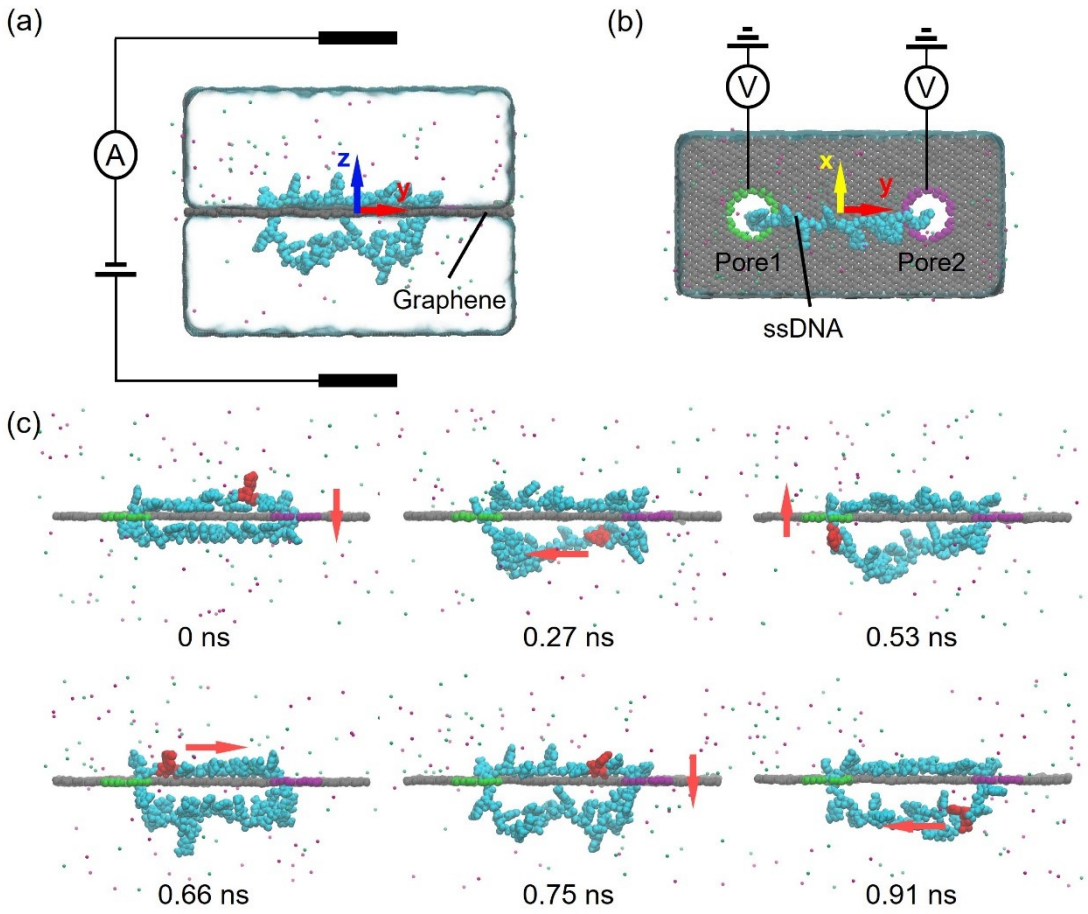

Figure S1 Schematic diagram of real-time analysis of bare ssDNA rotation at a voltage of 16V. The simulation system setup viewed from the side (a) and top (b). The colored nanopores indicate that they are positively (purple) or negatively (green) charged, the amplitude of nanopore surface charge density is 0.075 e/Å^2. (c) The rotation of the ssDNA at 0ns, 0.27ns, 0.53ns, 0.66ns, 0.75ns, and 0.91ns, the ssDNA completes nearly one cycle of rotation clockwise. The red mark on the

ssDNA strand is the residues that is intentionally marked to show the rotational state more clearly.

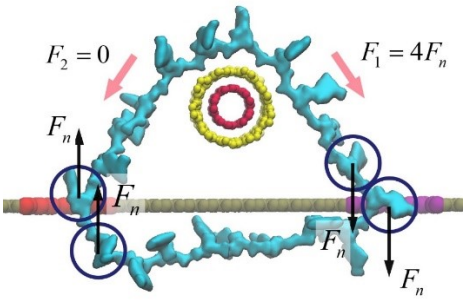

Figure S2 Schematic diagram of the calculation method of output power and torque of CNT nanomotor. To obtain the output parameters of the CNT nanomotor simplistically, we simplified the computational model. First, the electrophoretic force of ssDNA and the friction between ssDNA and nanopore were ignored, and only the electroosmotic force on two bases near the nanopore was considered. The electroosmotic force can be calculated by the Stokes friction equation.

$$F_n = 6\pi\eta r v \quad \textbf{(1)}$$

where η is the kinetic viscosity of the solution, r is the equivalent radius of the base, and v is the electroosmotic flow rate.

Then, we assume that the four bases near the two nanopores are subjected to equal magnitude of electroosmotic forces, and the tight-edge tension acting on the rotor is F_1=4F_n, and the loose-edge tension is F_1=0. Then the relationship between output power and torque is as follows:

$$P = (F_1 - F_2)v_{rot} = \frac{T}{R}v_{rot} \quad \textbf{(2)}$$

Where P is the output power of the nanomotor, T is the output torque of the nanomotor, R is the rotor radius, and v_{rot} is the speed of the nanomotor.

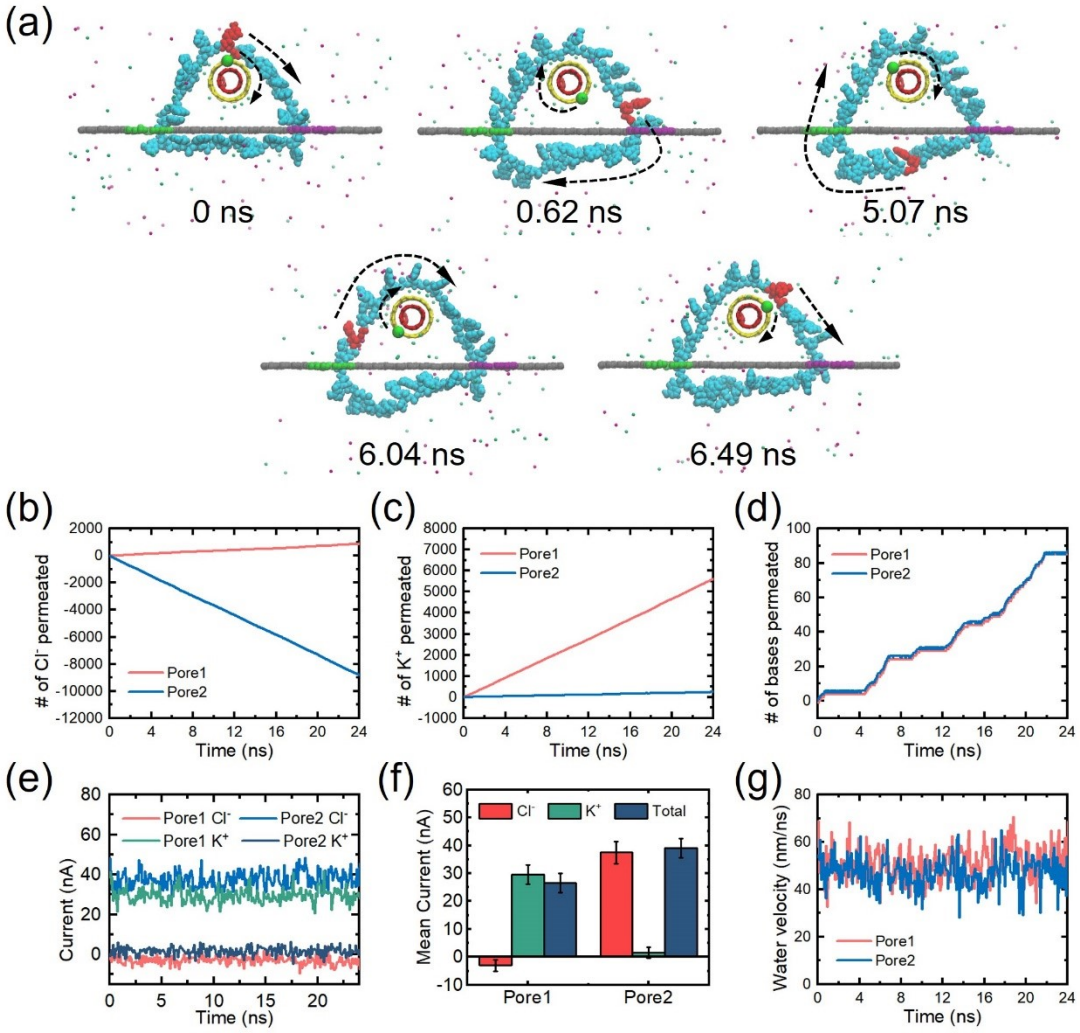

Figure S3 Schematic diagram of real-time analysis of CNT motor rotation at a voltage of 14V. (a) The rotation of the nanomotor at 0ns, 0.62ns, 5.07ns, 6.04ns, and 6.49ns, the motor completes nearly one cycle of rotation clockwise. The red marks on the ssDNA strand and the green marks on the rotor carbon tube are the residues and C atoms that are intentionally marked to show the rotational state more clearly. (b) Variation of the amount of Cl^- passing through the two nanopores with time. (a) Variation of the amount of K^+ passing through the two nanopores with time. (c) Variation of the amount of base passing through the two nanopores with time. (d) Real-time currents generated by Cl^- and K^- in the two nanopores. (e) Current contribution of two ions in two nanopores with different surface charge densities. (f) Fluctuations of the water velocity in the two nanopores.

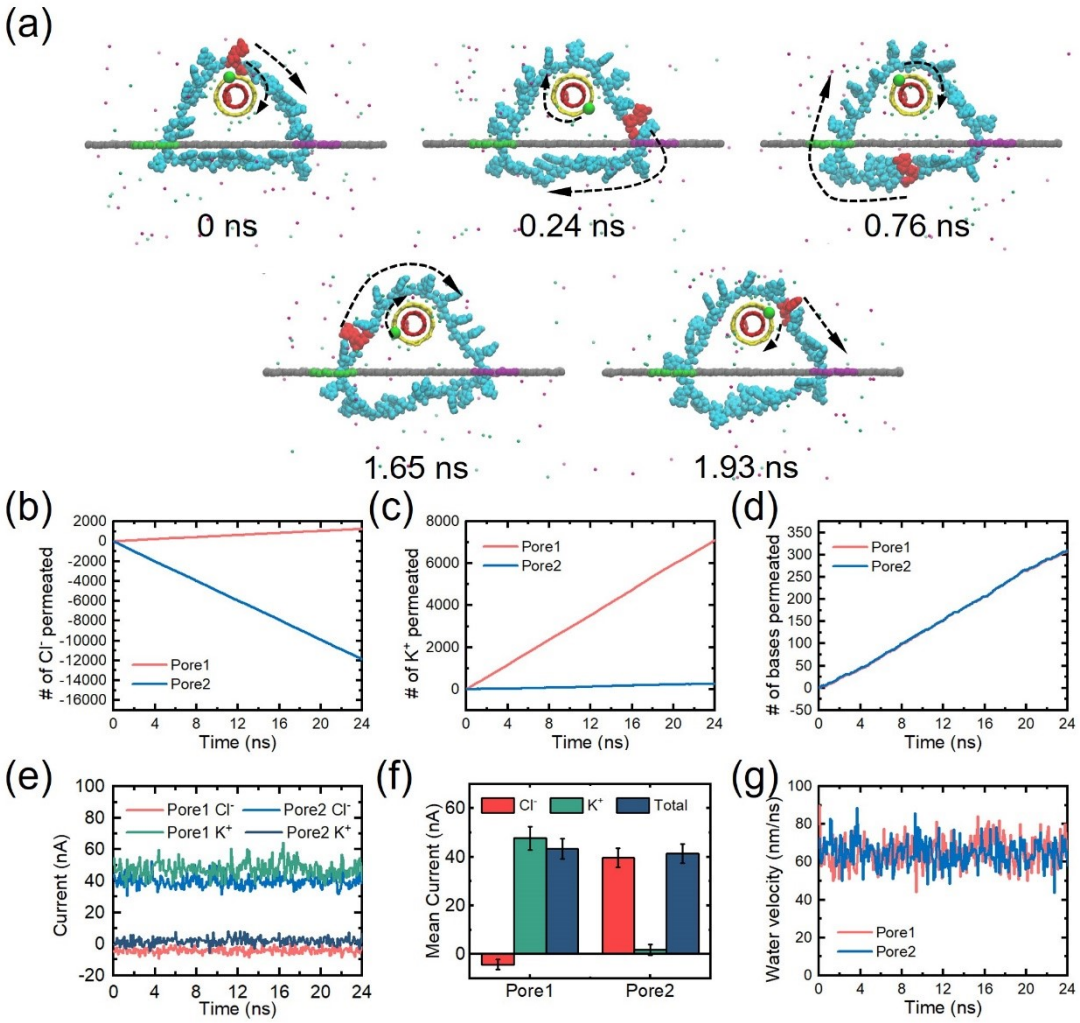

Figure S4 Schematic diagram of real-time analysis of CNT motor rotation at a voltage of 15V. (a) The rotation of the nanomotor at 0ns, 0.24ns, 0.76ns, 1.65ns, and 1.93ns, the motor completes nearly one cycle of rotation clockwise. The red marks on the ssDNA strand and the green marks on the rotor carbon tube are the residues and C atoms that are intentionally marked to show the rotational state more clearly. (b) Variation of the amount of Cl^- passing through the two nanopores with time. (a) Variation of the amount of K^+ passing through the two nanopores with time. (c) Variation of the amount of base passing through the two nanopores with time. (d) Real-time currents generated by Cl^- and K^- in the two nanopores. (e) Current contribution of two ions in two nanopores with different surface charge densities. (f) Fluctuations of the water velocity in the two nanopores.

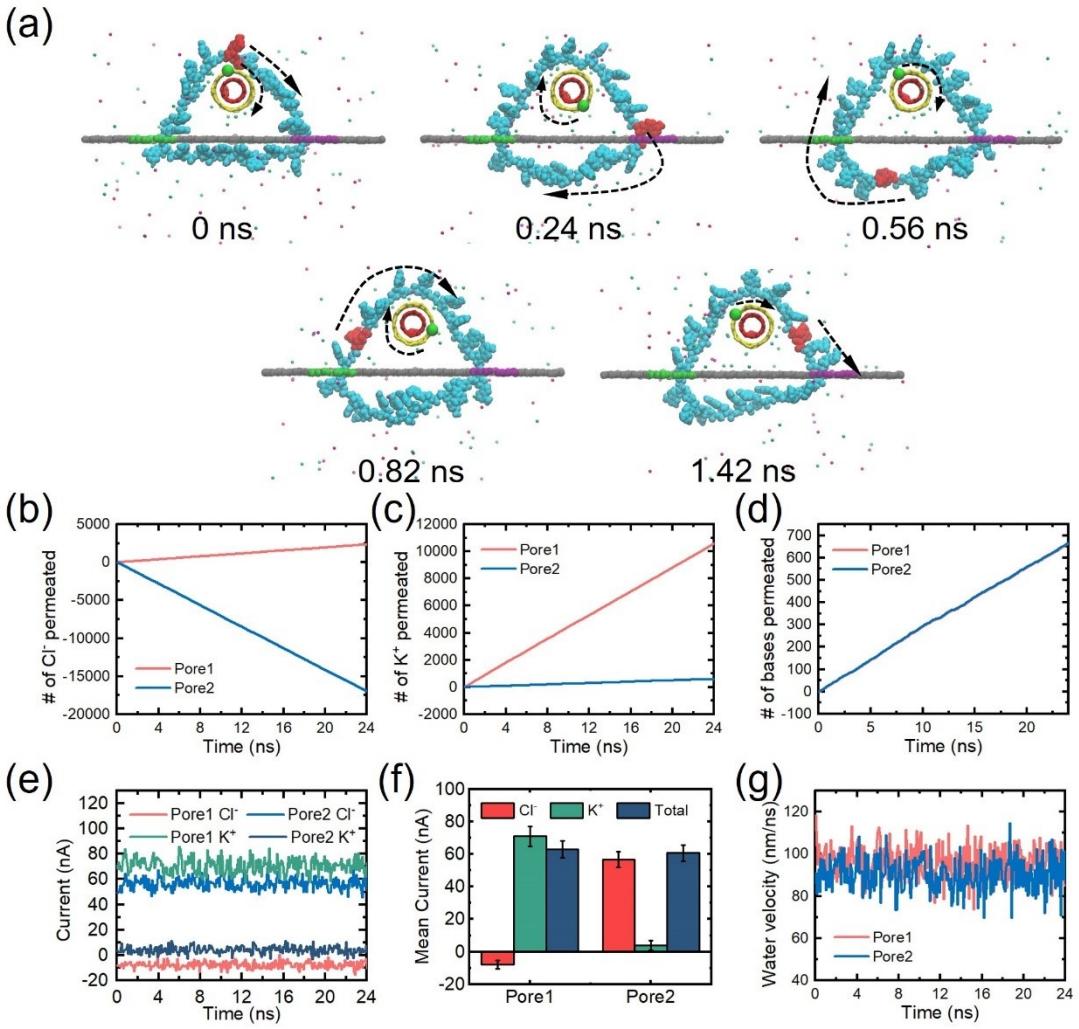

Figure S5 Schematic diagram of real-time analysis of CNT motor rotation at a voltage of 17V. (a) The rotation of the nanomotor at 0ns, 0.24ns, 0.56ns, 0.82ns, and 1.42ns, the motor completes nearly one cycle of rotation clockwise. The red marks on the ssDNA strand and the green marks on the rotor carbon tube are the residues and C atoms that are intentionally marked to show the rotational state more clearly. (b) Variation of the amount of Cl^- passing through the two nanopores with time. (a) Variation of the amount of K^+ passing through the two nanopores with time. (c) Variation of the amount of base passing through the two nanopores with time. (d) Real-time currents generated by Cl^- and K^- in the two nanopores. (e) Current contribution of two ions in two nanopores with different surface charge densities. (f) Fluctuations of the water velocity in the two nanopores.

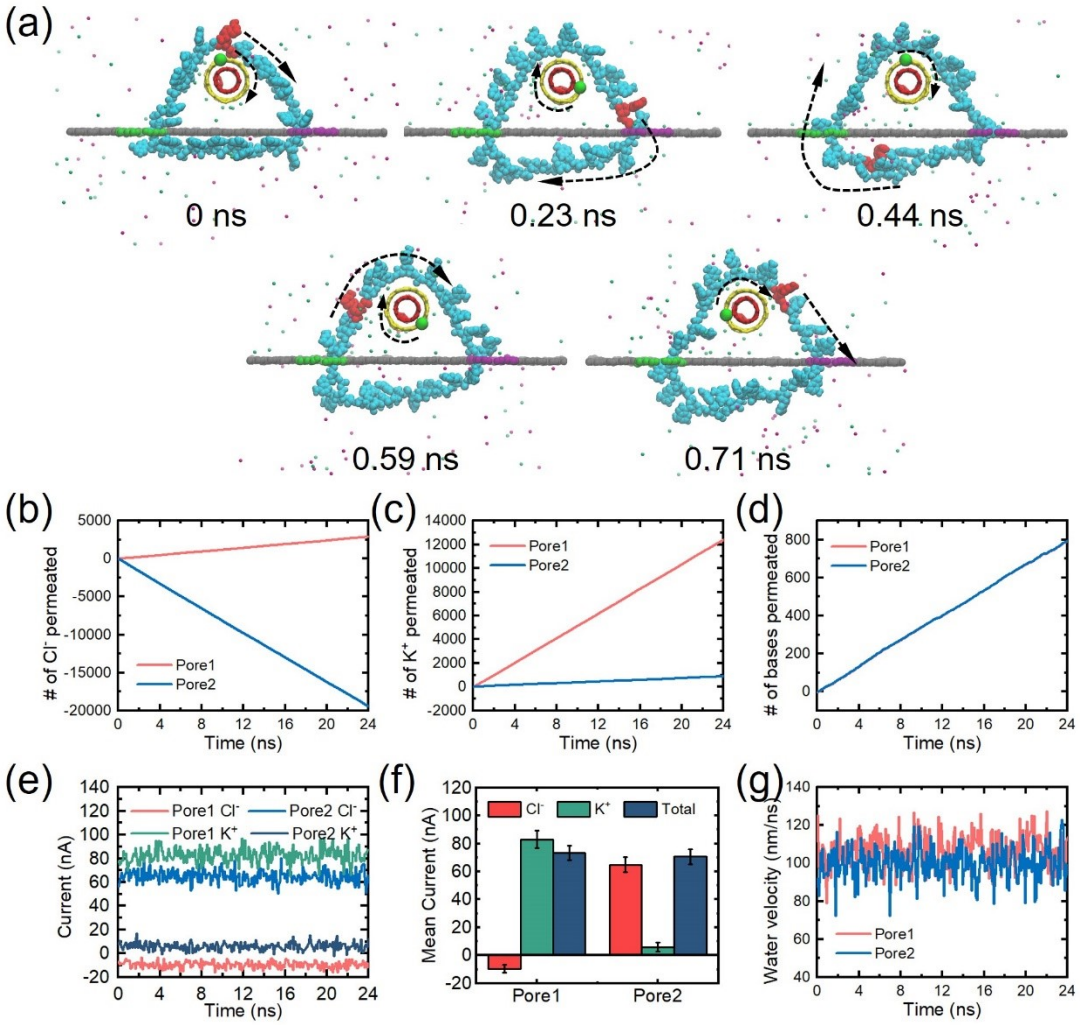

Figure S6 Schematic diagram of real-time analysis of CNT motor rotation at a voltage of 18V. (a) The rotation of the nanomotor at 0ns, 0.23ns, 0.44ns, 0.59ns, and 0.71ns, the motor completes nearly one cycle of rotation clockwise. The red marks on the ssDNA strand and the green marks on the rotor carbon tube are the residues and C atoms that are intentionally marked to show the rotational state more clearly. (b) Variation of the amount of Cl^- passing through the two nanopores with time. (a) Variation of the amount of K^+ passing through the two nanopores with time. (c) Variation of the amount of base passing through the two nanopores with time. (d) Real-time currents generated by Cl^- and K^- in the two nanopores. (e) Current contribution of two ions in two nanopores with different surface charge densities. (f) Fluctuations of the water velocity in the two nanopores.

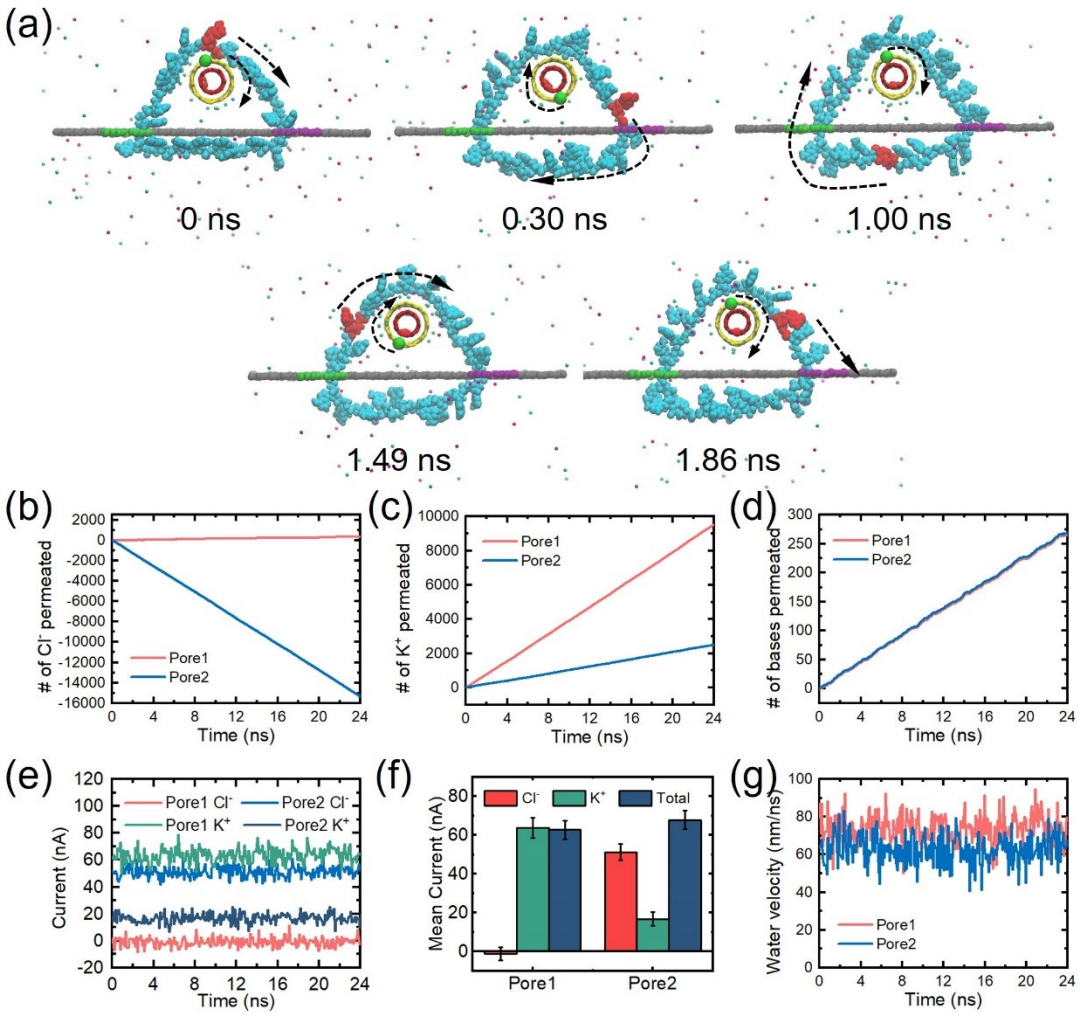

Figure S7 Schematic diagram of real-time analysis of CNT motor rotation at a surface charge density of 0.049 e/Å^2. (a) The rotation of the nanomotor at 0ns, 0.30ns, 1.00ns, 1.49ns, and 1.86ns, the motor completes nearly one cycle of rotation clockwise. The red marks on the ssDNA strand and the green marks on the rotor carbon tube are the residues and C atoms that are intentionally marked to show the rotational state more clearly. (b) Variation of the amount of Cl^- passing through the two nanopores with time. (a) Variation of the amount of K^+ passing through the two nanopores with time. (c) Variation of the amount of base passing through the two nanopores with time. (d) Real-time currents generated by Cl^- and K^- in the two nanopores. (e) Current contribution of two ions in two nanopores with different surface charge densities. (f) Fluctuations of the water velocity in the two nanopores.

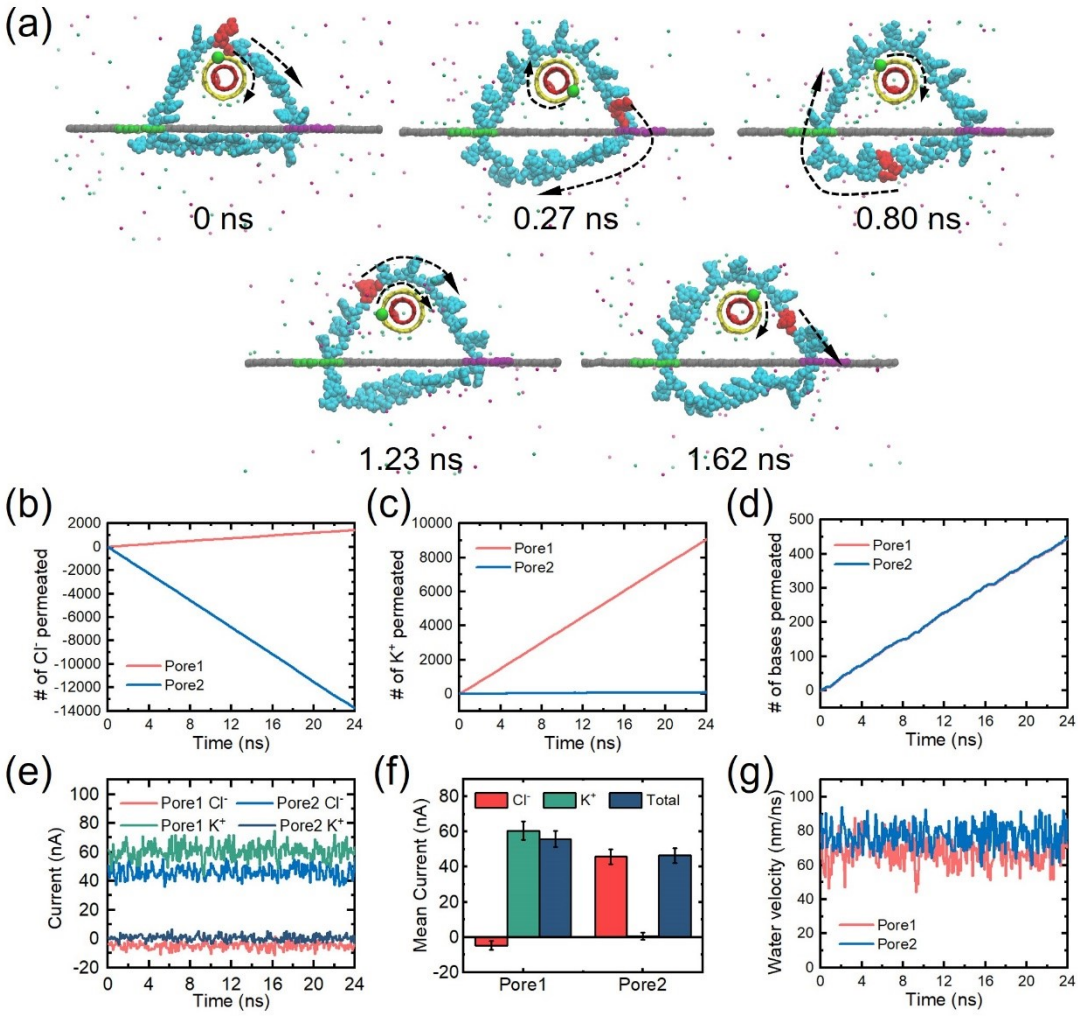

Figure S8 Schematic diagram of real-time analysis of CNT motor rotation at a surface charge density of 0.102 e/Å^2. (a) The rotation of the nanomotor at 0ns, 0.27ns, 0.80ns, 1.23ns, and 1.62ns, the motor completes nearly one cycle of rotation clockwise. The red marks on the ssDNA strand and the green marks on the rotor carbon tube are the residues and C atoms that are intentionally marked to show the rotational state more clearly. (b) Variation of the amount of Cl^- passing through the two nanopores with time. (a) Variation of the amount of K^+ passing through the two nanopores with time. (c) Variation of the amount of base passing through the two nanopores with time. (d) Real-time currents generated by Cl^- and K^- in the two nanopores. (e) Current contribution of two ions in two nanopores with different surface charge densities. (f) Fluctuations of the water velocity in the two nanopores.

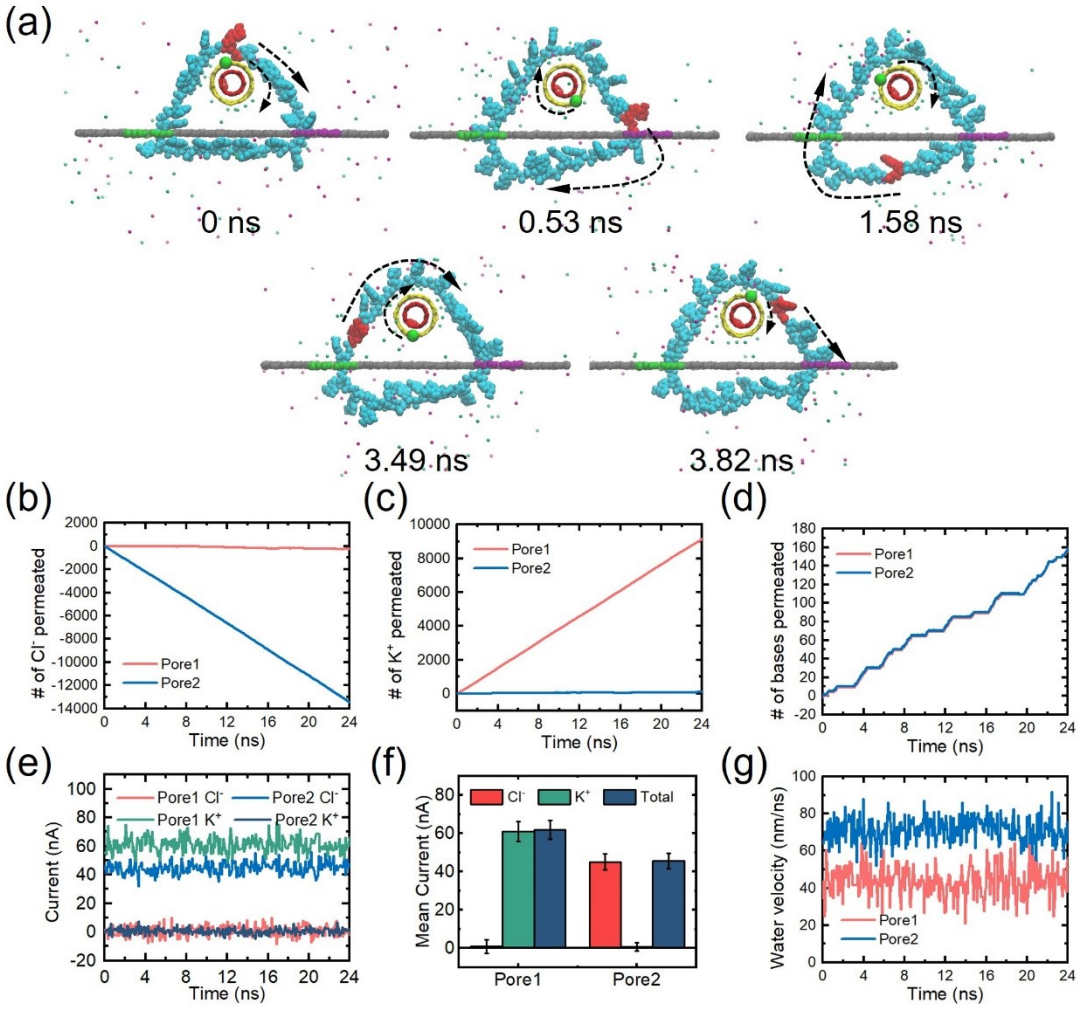

Figure S9 Schematic diagram of real-time analysis of CNT motor rotation at a surface charge density of 0.127 e/Å^2. (a) The rotation of the nanomotor at 0ns, 0.53ns, 1.58ns, 3.49ns, and 3.86ns, the motor completes nearly one cycle of rotation clockwise. The red marks on the ssDNA strand and the green marks on the rotor carbon tube are the residues and C atoms that are intentionally marked to show the rotational state more clearly. (b) Variation of the amount of Cl^- passing through the two nanopores with time. (a) Variation of the amount of K^+ passing through the two nanopores with time. (c) Variation of the amount of base passing through the two nanopores with time. (d) Real-time currents generated by Cl^- and K^- in the two nanopores. (e) Current contribution of two ions in two nanopores with different surface charge densities. (f) Fluctuations of the water velocity in the two nanopores.

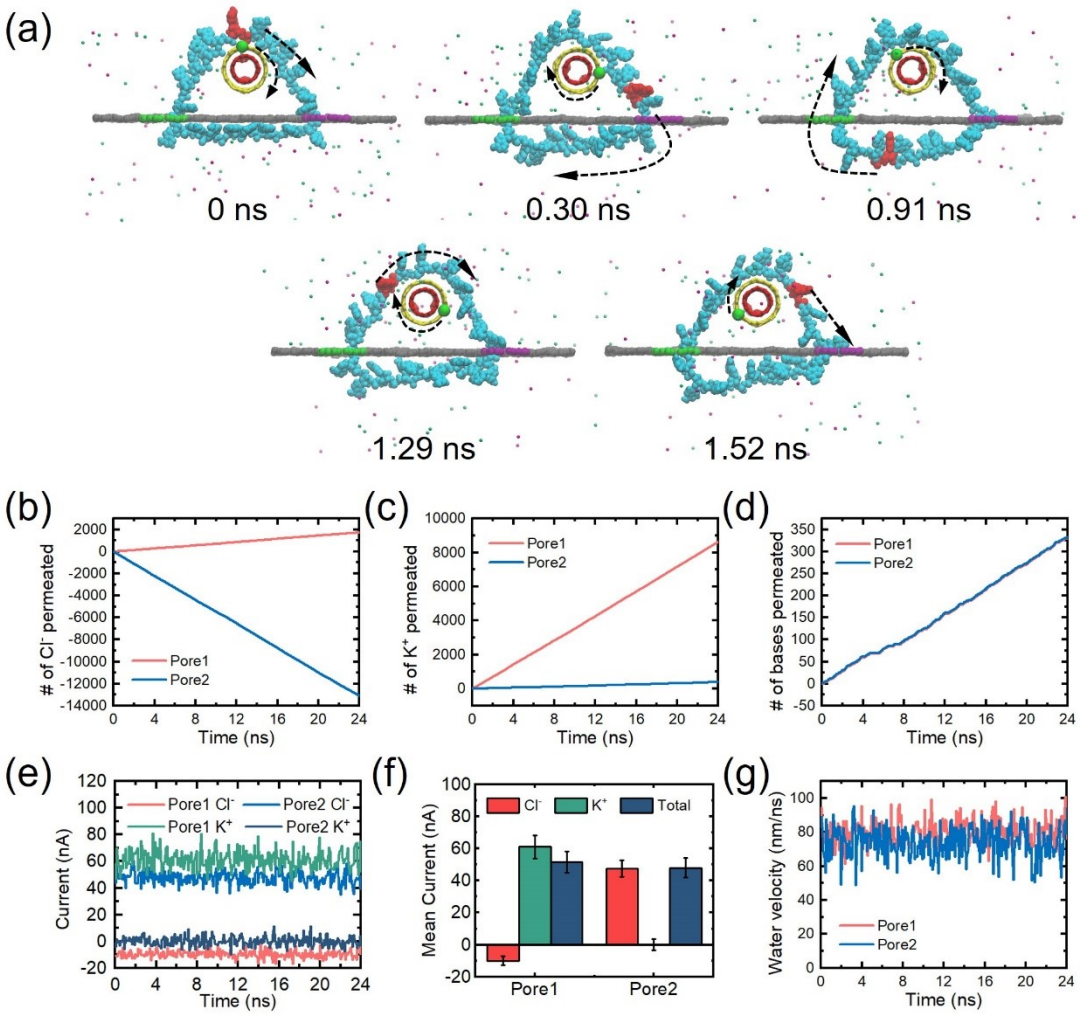

Figure S10 Schematic diagram of real-time analysis of CNT motor rotation at a rotor radius of 6.755 Å. (a) The rotation of the nanomotor at 0ns, 0.30ns, 0.91ns, 1.29ns, and 1.52ns, the motor completes nearly one cycle of rotation clockwise. The red marks on the ssDNA strand and the green marks on the rotor carbon tube are the residues and C atoms that are intentionally marked to show the rotational state more clearly. (b) Variation of the amount of Cl^- passing through the two nanopores with time. (a) Variation of the amount of K^+ passing through the two nanopores with time. (c) Variation of the amount of base passing through the two nanopores with time. (d) Real-time currents generated by Cl^- and K^- in the two nanopores. (e) Current contribution of two ions in two nanopores with different surface charge densities. (f) Fluctuations of the water velocity in the two nanopores.

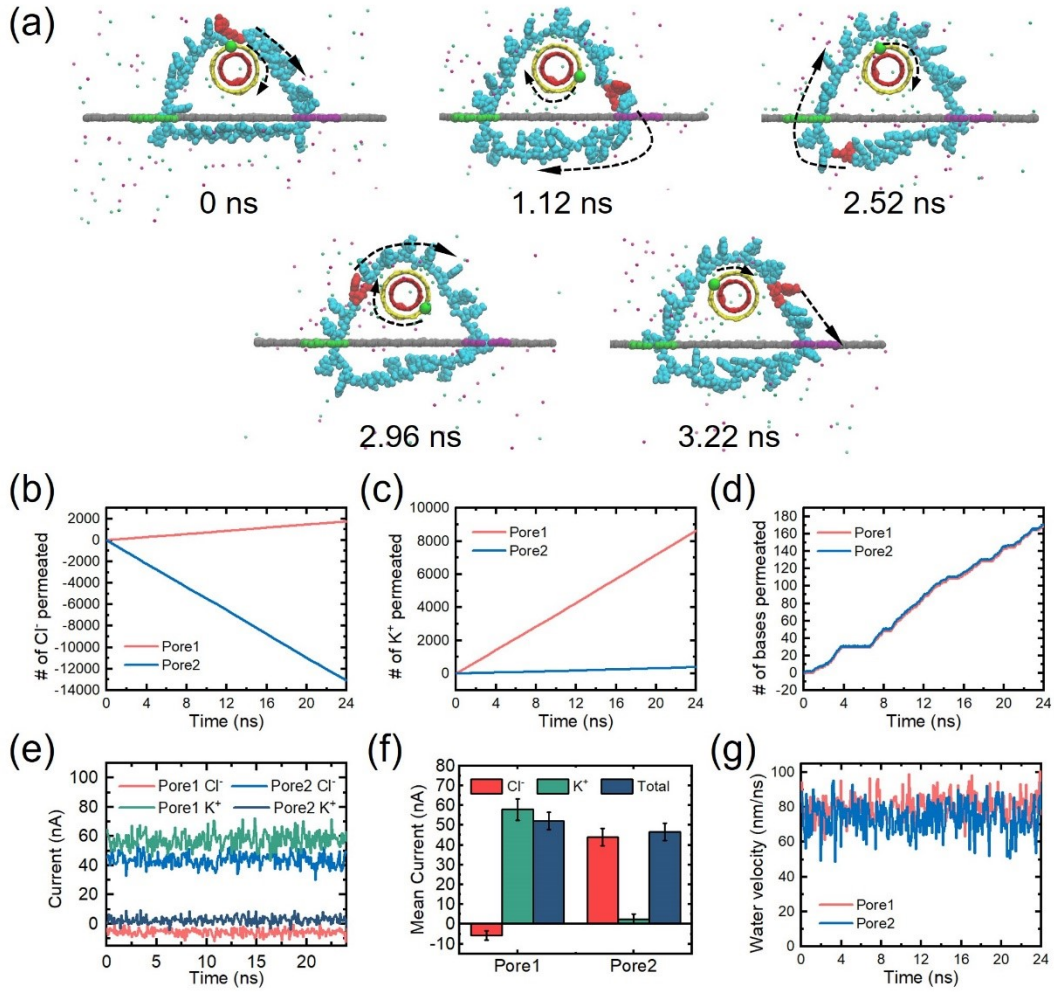

Figure S11 Schematic diagram of real-time analysis of CNT motor rotation at a rotor radius of 7.430 Å. (a) The rotation of the nanomotor at 0ns, 1.12ns, 2.52ns, 2.96ns, and 3.22ns, the motor completes nearly one cycle of rotation clockwise. The red marks on the ssDNA strand and the green marks on the rotor carbon tube are the residues and C atoms that are intentionally marked to show the rotational state more clearly. (b) Variation of the amount of Cl^- passing through the two nanopores with time. (a) Variation of the amount of K^+ passing through the two nanopores with time. (c) Variation of the amount of base passing through the two nanopores with time. (d) Real-time currents generated by Cl^- and K^- in the two nanopores. (e) Current contribution of two ions in two nanopores with different surface charge densities. (f) Fluctuations of the water velocity in the two nanopores.

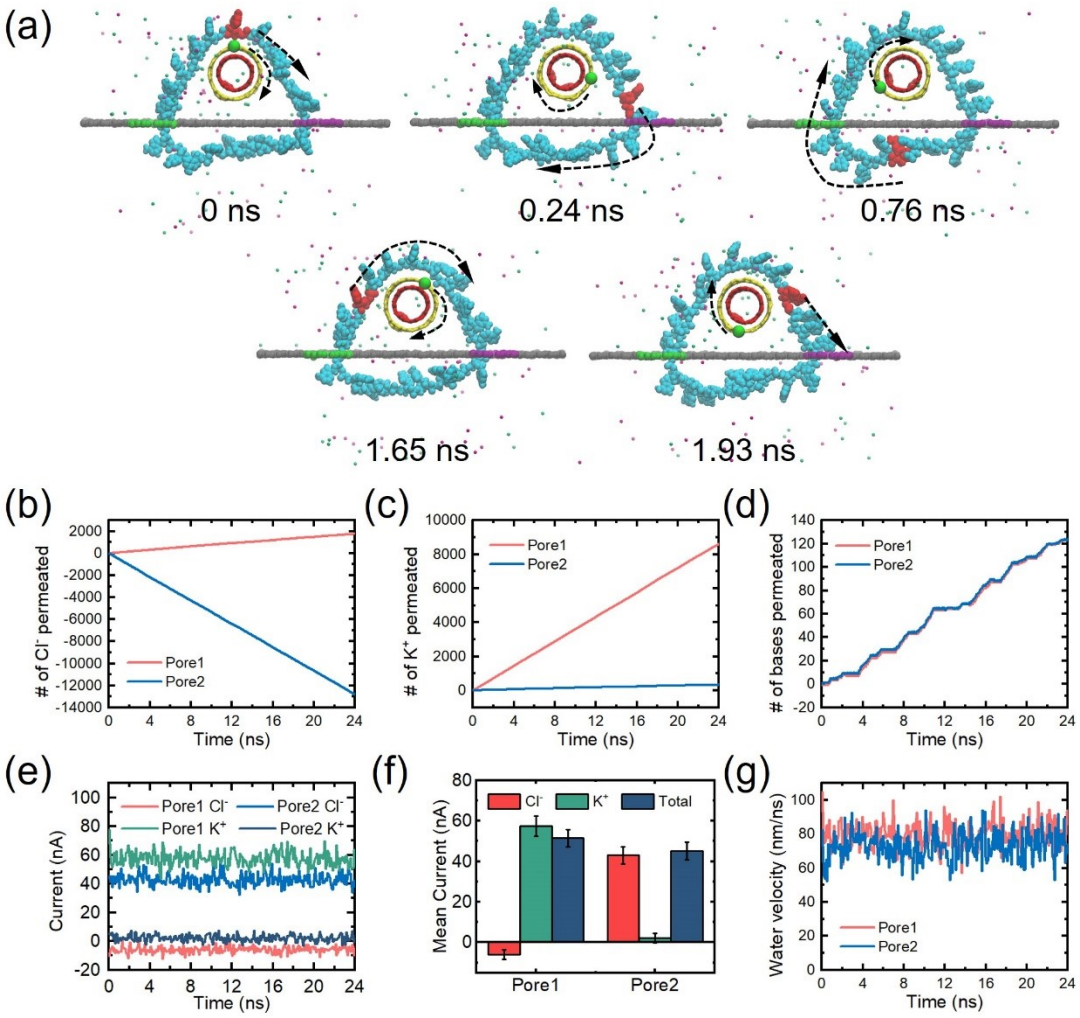

Figure S12 Schematic diagram of real-time analysis of CNT motor rotation at a rotor radius of 8.106 Å. (a) The rotation of the nanomotor at 0ns, 0.24ns, 0.76ns, 1.65ns, and 1.93ns, the motor completes nearly one cycle of rotation clockwise. The red marks on the ssDNA strand and the green marks on the rotor carbon tube are the residues and C atoms that are intentionally marked to show the rotational state more clearly. (b) Variation of the amount of Cl^- passing through the two nanopores with time. (a) Variation of the amount of K^+ passing through the two nanopores with time. (c) Variation of the amount of base passing through the two nanopores with time. (d) Real-time currents generated by Cl^- and K^- in the two nanopores. (e) Current contribution of two ions in two nanopores with different surface charge densities. (f) Fluctuations of the water velocity in the two nanopores.

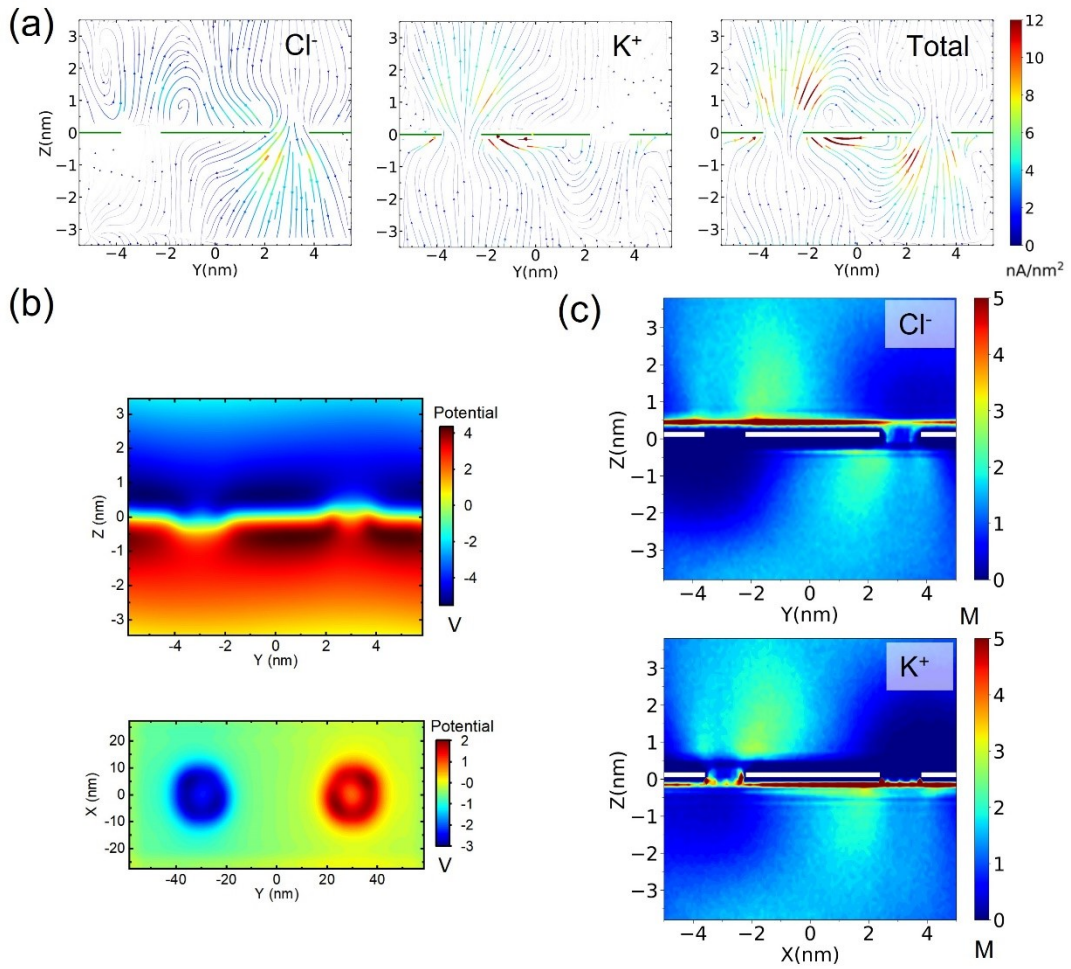

Figure S13 Selective ion transport through the nanopores at a voltage of 14V. (a) The steady-state ionic current densities and flux maps for Cl^- and K^+ and Total on the Y–Z cross-section. The arrows and the colors indicate the directions and magnitudes of the flux, respectively. (b) The 2D potential distributions on the Y-Z plane and X-Y plane that pass through the top and bottom shown in panel (c) The local ion concentration distribution of Cl^- and K^+ on the Y–Z cross-section.

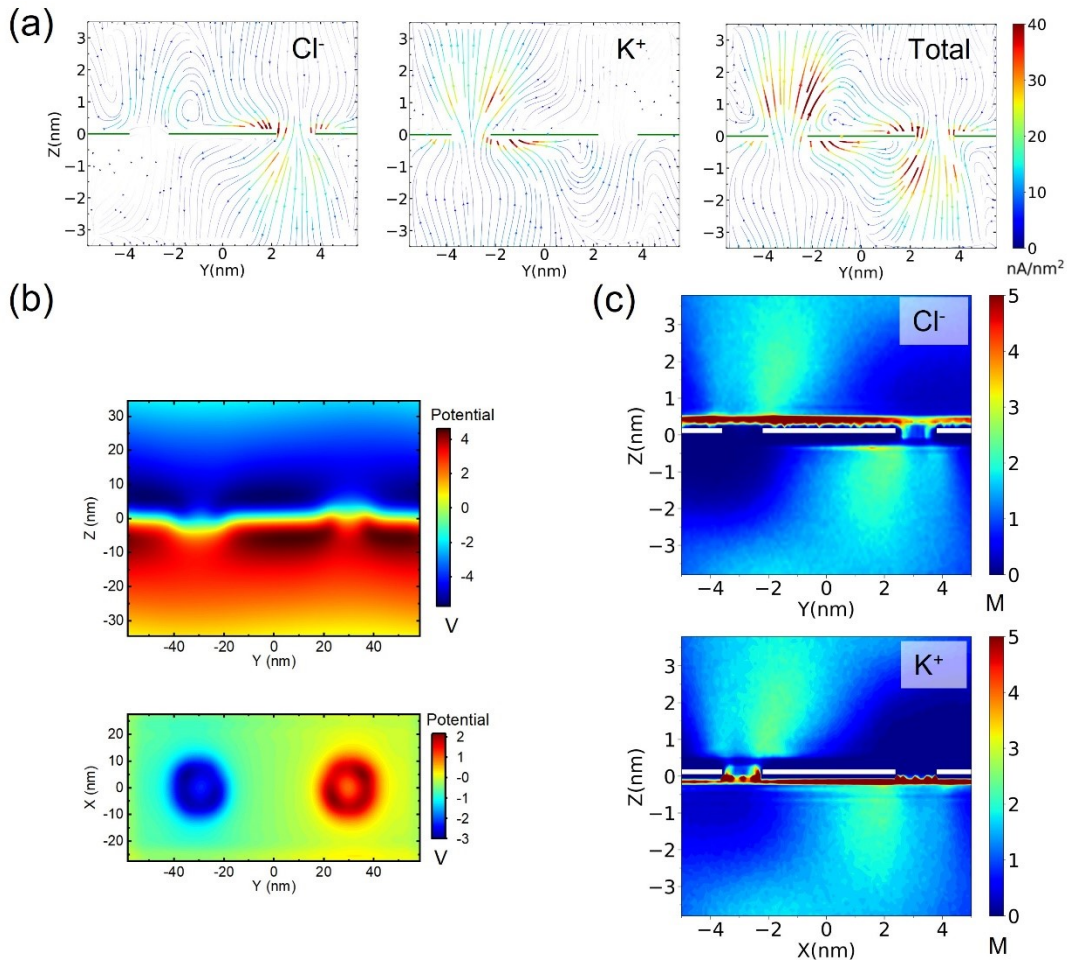

Figure S14 Selective ion transport through the nanopores at a voltage of 15V. (a) The steady-state ionic current densities and flux maps for Cl^- and K^+ and Total on the Y–Z cross-section. The arrows and the colors indicate the directions and magnitudes of the flux, respectively. (b) The 2D potential distributions on the Y-Z plane and X-Y plane that pass through the top and bottom shown in panel (c) The local ion concentration distribution of Cl^- and K^+ on the Y–Z cross-section.

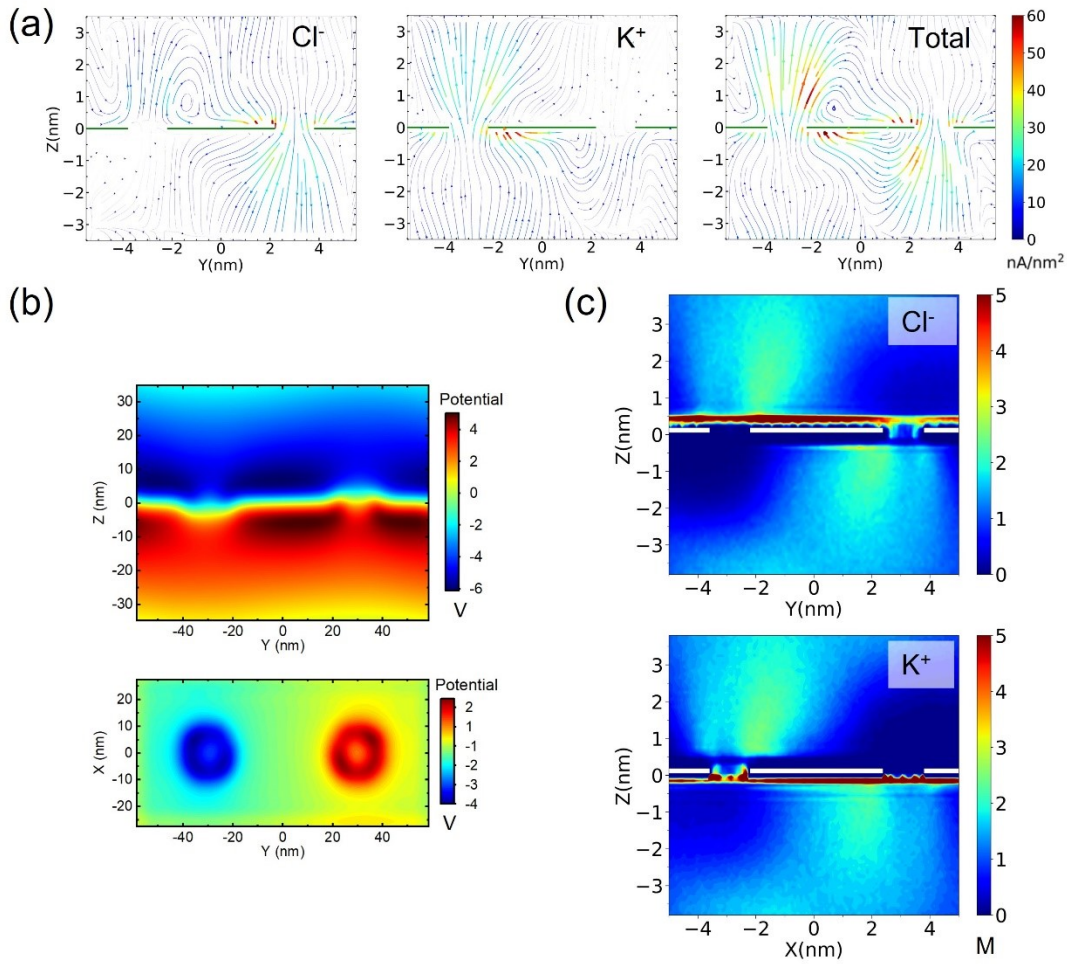

Figure S15 Selective ion transport through the nanopores at a voltage of 17V. (a) The steady-state ionic current densities and flux maps for Cl^- and K^+ and Total on the Y–Z cross-section. The arrows and the colors indicate the directions and magnitudes of the flux, respectively. (b) The 2D potential distributions on the Y-Z plane and X-Y plane that pass through the top and bottom shown in panel (c) The local ion concentration distribution of Cl^- and K^+ on the Y–Z cross-section.

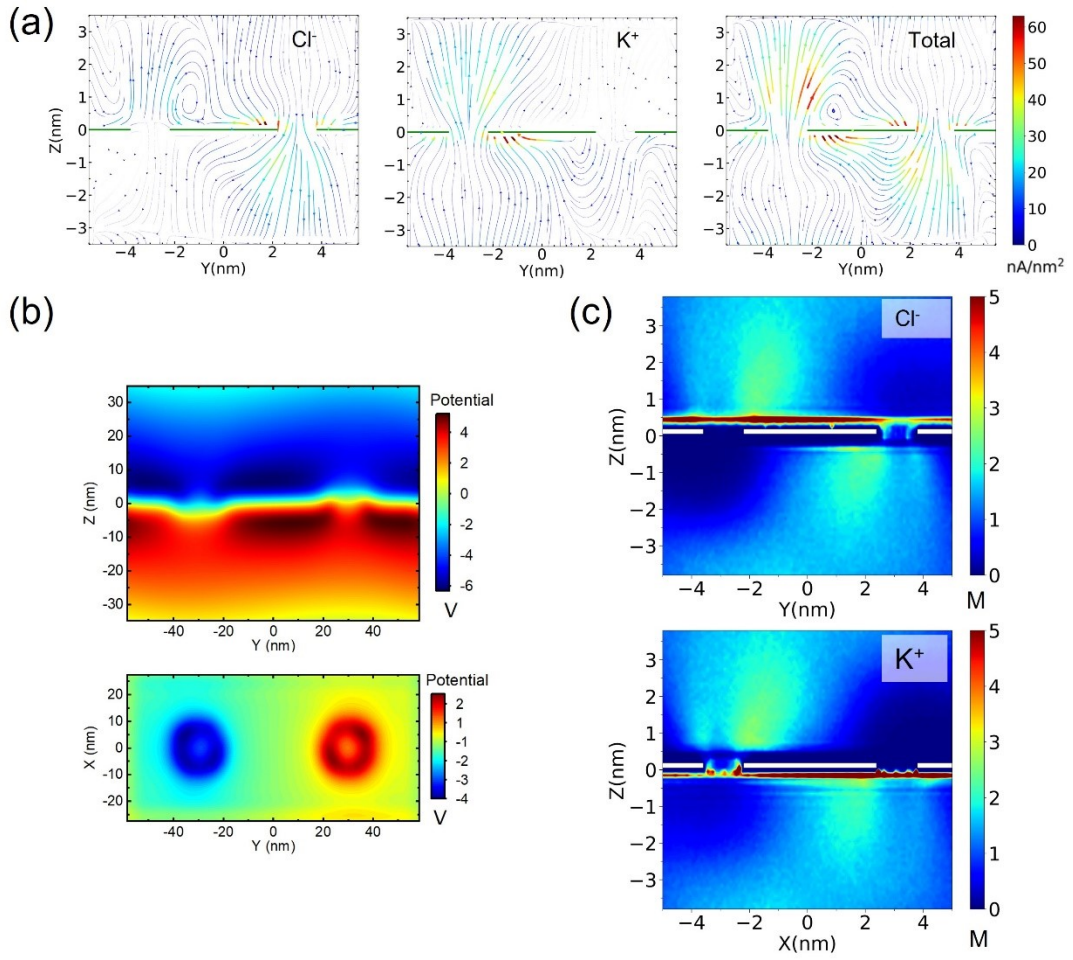

Figure S16 Selective ion transport through the nanopores at a voltage of 18V. (a) The steady-state ionic current densities and flux maps for Cl^- and K^+ and Total on the Y–Z cross-section. The arrows and the colors indicate the directions and magnitudes of the flux, respectively. (b) The 2D potential distributions on the Y-Z plane and X-Y plane that pass through the top and bottom shown in panel (c) The local ion concentration distribution of Cl^- and K^+ on the Y–Z cross-section.

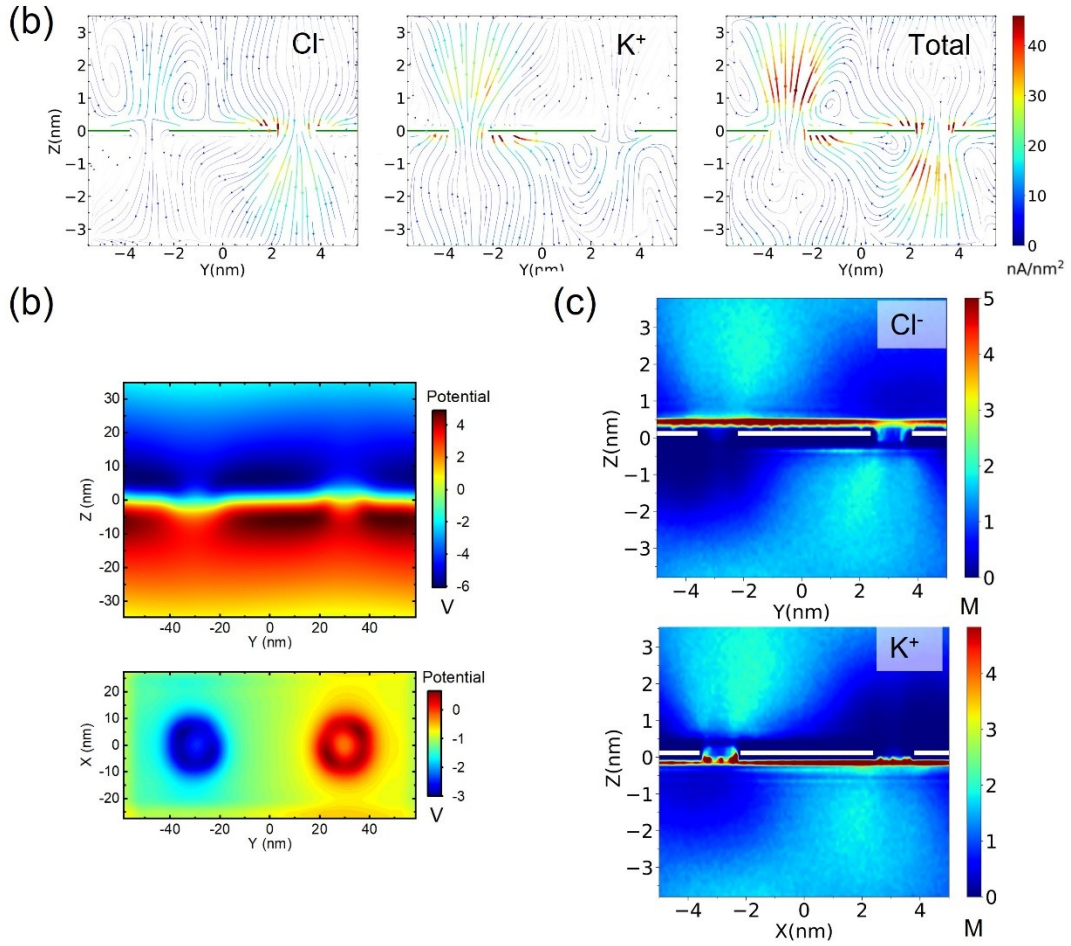

Figure S17 Selective ion transport through the nanopores at a surface charge density of 0.049 e/Å^2. (a) The steady-state ionic current densities and flux maps for Cl^- and K^+ and Total on the Y–Z cross-section. The arrows and the colors indicate the directions and magnitudes of the flux, respectively. (b) The 2D potential distributions on the Y-Z plane and X-Y plane that pass through the top and bottom shown in panel (c) The local ion concentration distribution of Cl^- and K^+ on the Y–Z cross-section.

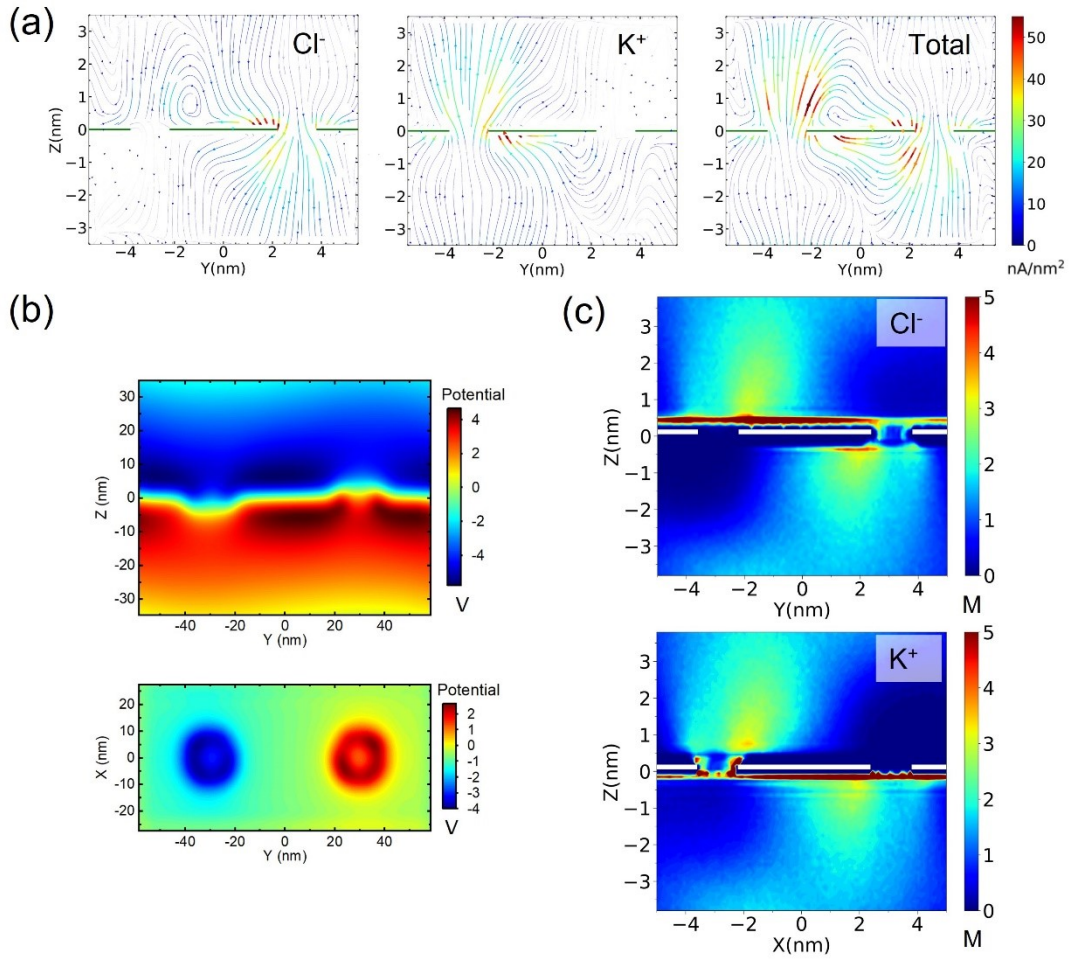

Figure S18 Selective ion transport through the nanopores at a surface charge density of 0.102 e/Å^2. (a) The steady-state ionic current densities and flux maps for Cl^- and K^+ and Total on the Y–Z cross-section. The arrows and the colors indicate the directions and magnitudes of the flux, respectively. (b) The 2D potential distributions on the Y-Z plane and X-Y plane that pass through the top and bottom shown in panel (c) The local ion concentration distribution of Cl^- and K^+ on the Y–Z cross-section.

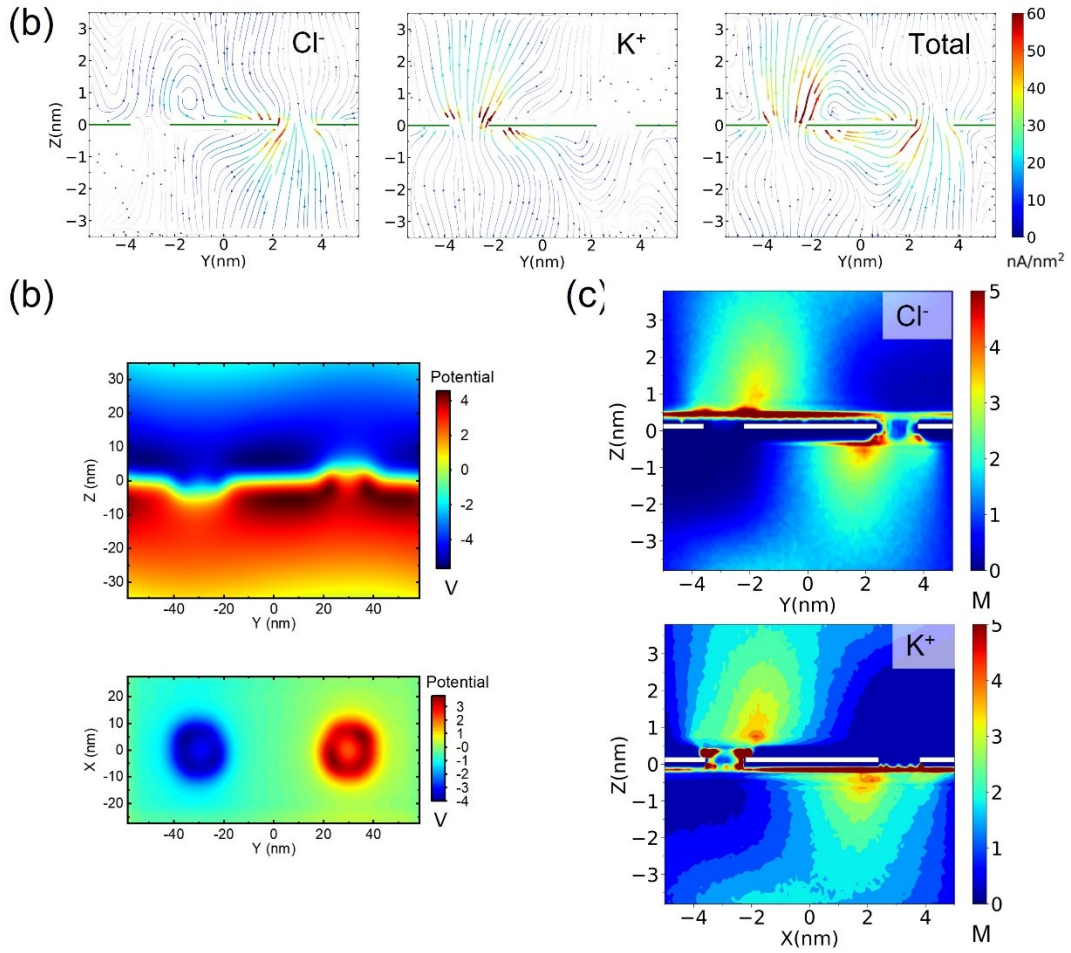

Figure S19 Selective ion transport through the nanopores at a surface charge density of 0.127 e/Å^2. (a) The steady-state ionic current densities and flux maps for Cl^- and K^+ and Total on the Y–Z cross-section. The arrows and the colors indicate the directions and magnitudes of the flux, respectively. (b) The 2D potential distributions on the Y-Z plane and X-Y plane that pass through the top and bottom shown in panel (c) The local ion concentration distribution of Cl^- and K^+ on the Y–Z cross-section.